Hindawi
International Journal of Antennas and Propagation
Volume 2022, Article ID 1951162, 12 pages
https://doi.org/10.1155/2022/1951162

Research Article

Study on Numerical Simulation and Electromagnetic Scattering of Time-Invariant Freak Waves

Lichen Han, Gengkun Wu, and Bin Liu

College of Computer Science and Engineering, Shandong University of Science and Technology, Qingdao 266590, Shandong, China

Correspondence should be addressed to Gengkun Wu; wugengkun@sdust.edu.cn

Received 4 January 2022; Revised 11 August 2022; Accepted 2 September 2022; Published 20 September 2022

Academic Editor: Hervé Aubert

The occurrence probability of freak waves is related to the sea wave spectrum. In this paper, different wave spectrums are used to simulate time-invariant three-dimensional freak waves. Freak waves that meet the international standards are generated at fixed time and location by adjusting the energy of the wavelets. We studied the occurrence probability of freak waves under the conditions of different wave spectrums, different wind speeds, and different modulation ratios and optimized the calculation speed of the model. Simulation data show that the difference in the shape of the wave spectrum affects the probability of freak waves occurrence. The model conforms to the Benjamin–Feir index (BFI), and the ratio of wave steepness to spectrum bandwidth is the key. In this paper, the Kirchhoff approximation theory is used to study the electromagnetic scattering (EM scattering) properties of freak waves on the large scale. We ideally calculate the Normalized Radar Cross-Section (NRCS) from the sea surface with freak waves, under different wind speeds and different grazing angles. The NRCS of freak waves is extremely low, and the increase of wind speed and the decrease of the grazing angle will make the detection of freak waves more difficult. The possibility of detection of freak waves is higher at high grazing angles (low incidence angles). The numerical simulations provide reference for engineering.

1. Introduction

Freak waves are abnormally large-amplitude waves that appear suddenly from nowhere in different regions of the world ocean. This dangerous natural phenomenon unusually lasts for tens of seconds, and it is difficult to obtain complete and long-term observation data [1–3]. It is practically impossible for a ship's crew to take any precaution measures to prevent freak waves with wave heights of 10 ~ 30 meters. These waves can pose devastating damage on ships and marine structures and have a serious impact on the offshore industry [4–6]. Such extreme ocean phenomena have been extensively studied. The main contents of the theoretical part include definition, genesis, observation and record, numerical analysis, and simulation. In terms of application, the prevention of the hazard of freak waves is an important topic. Wave force under freak waves is a conventional and at the same time very frontier problem [7]. The early warning and forecasting of freak waves are also very important [8, 9].

The mechanisms of freak waves generation are still under discussion. Freak waves can appear in extreme sea conditions and can suddenly appear in normal seas. Many mechanisms have been proposed to explain these rogue waves [10]. Wave focusing: Wave energy may be concentrated in a small area because of wave trapping, refraction, and reflection, such as wave–current interaction; wind force; bottom topography influence, etc. [11–13]. The modulation instability, also known as Benjamin-Feir instability [14], has been accepted by many researchers to explain the occurrence of freak waves. Benjamin-Feir instability has achieved good results in experimental studies [15, 16]. New mechanisms are constantly being proposed to explain this extreme phenomenon. For example, Fedele [17] questioned the modulational instability, arguing that freak waves are likely to be rare occurrences of weakly nonlinear random seas. Various studies on freak waves have been developing. For example, Lavrenov studied freak waves with deep trough [18]; L. Zou studied the rapid variation of water depth, such as slope and

seamount, contributing to the occurrence probability of freak waves [19]; Takuji Waseda studied the relationship between freak waves and spectral [20]; Babanin studied the modulational instability, steepness, and spectral bandwidth [21, 22]. Exploring the generation mechanism of freak waves depends on the progress of experimental equipment and further research.

Numerical simulation is an important part of the study of freak waves and has practical application value. Numerical simulation methods: the linear wave superposition theory; the nonlinear Schrödinger (NLS) equation; computational fluid dynamics (CFD) based on viscous flow theory; Korteweg–de Vries (KdV) equation, and Kadomtsev–Petviashvili (KP) equation, etc. [23]. The key point of this paper is to reduce the amount of calculation, improve the calculation efficiency, and quickly simulate the freak waves. The linear wave focusing method is chosen to simulate the freak waves.

More attention has been paid in the study of EM scattering from rough sea surface. Obtaining marine information and target feature information through microwave remote sensing technology is meaningful for marine remote sensing, marine target detection, and identification, etc. For random rough sea surface, the strength of EM scattering ability (usually EM backscattering) has commonly used the scattering coefficient (or normalized radar cross-section, NRCS). There are many methods to calculate EM scattering from random sea surfaces, which can be divided into numerical methods and approximate methods. The former includes FDTD (Finite Difference Time Domain) [24], MoM (Method of Moment) [25], etc., while the latter includes KA (Kirchhoff Approximation) [26], SPM (Small Perturbation Method) [27], SSA (Small Slope Approximation) [28], TSM (Two-Scale Model) [29], etc.

The sea surface is a time-variant random rough surface, which will lead to many difficulties. In fact, it is difficult for current observation instruments to distinguish between noise and freak waves in the case of extreme sea conditions, due to the influence of droplets, foam, inherent noise of radar, and so on. Observational data show that most of the freak waves have noise characteristics, which makes the recording and research of the freak waves more difficult. This requires the development of wave observation instruments. Numerical simulations can ideally study time-invariant freak waves, ignoring complex environmental factors. The numerical simulation of electromagnetic scattering from sea surface is not affected by sea clutter, and the calculation speed is fast. The disadvantage is that the accuracy is not enough, which is different from the engineering project. Although it cannot be directly applied to engineering projects, the preliminary study of EM scattering of freak waves in theory can provide reference for solving practical problems.

In this paper, an ideal sea surface model with freak waves is established to study the EM scattering of freak waves. Freak waves are larger gravity waves. We study the approximate simulation of freak waves without considering the influence of surface tension on the spectrum, which can improve the calculation efficiency while maintaining the characteristics of freak waves. PM spectrum, JONSWAP spectrum, WEN spectrum, etc., can describe fully developed wind-driven sea surface and are suitable for simulating gravity waves. Based on the comparison of different wave spectra, JONSWAP wave spectrum and SWOP directional function are selected to simulate the random sea surface, and the freak waves are generated at fixed time and location on the sea surface. The freak waves simulated by JONSWAP spectrum is a sea surface with obvious macroscopic features. Small-scale waves ranging from a few centimeters to tens of centimeters and millimeter droplets have little effect on the numerical simulation. For the above reasons, without discussing the microwave scattering from the sea surface, this paper uses the Kirchhoff approximation method in the study of EM scattering from random sea surface to establish the EM backscattering model. We study the EM scattering from the freak waves under the condition of analytical approximation and compare the backscattering coefficient (NRCS) of freak waves and background waves.

2. Numerical Simulation of Freak Waves Based on Different Wave Spectra

The notion of freak waves was first introduced by Drapper (1965) [30], and extremely large-amplitude waves is its obvious feature. Klinting and Sand (1987) [31] proposed a definition of freak waves including three conditions:

(1) $D_1 : H_0/H_s \geq 2.$

(2) $D_2 : \eta/H_0 \geq 0.65.$

(3) $D_3 : H_0/H_{0-1} \geq 2, D_4 : H_0/H_{0+1} \geq 2.$

The wave height H_0 of a freak wave is 2 times greater than the significant wave height H_s. The height of the freak wave crest η is greater than or equal to 0.65 times the wave height of this freak wave. H_0 is greater than or equal to 2 times the wave heights of two adjacent waves H_{0-1} and H_{0+1}. The definition of freak waves includes wave height, the relationship between adjacent wave heights, and the relationship between crests and troughs. Accurate definition is the key to distinguish freak waves from common extreme waves. But there is no widely accepted new definition so far. This paper will generate freak waves that meet the above general definition $D_1 \sim D_4$.

2.1. Three Kinds of Sea Wave Spectra. In this paper, the wave height is obtained by

$$\zeta(x, y, t) = \sum_{m=1}^{M} \sum_{n=1}^{N} A_{mn} \cos\left(\omega_m t - k_m x cos\theta_n - k_m \sin\theta_n + \varphi_{mn}\right)\#. \quad (1)$$

A_{mn} is the amplitude of the wavelet, ω_m is the angular frequency, k_m is the wave number, θ_n is the direction angle $[-\pi/2, \pi/2]$, and φ_{mn} is the random initial phase $(0, 2\pi)$.

$A_{mn} = \sqrt{2S(\omega,\theta)\Delta\omega\Delta\theta}$. $S(\omega,\theta) = S(\omega)G(\omega,\theta)$. $S(\omega)$ and $G(\omega,\theta)$ are the sea spectrum and the directional spectrum, respectively. The sea wave spectrum describes the distribution of the energy inside the wave with respect to frequency and direction. Common wave spectra include Elfouhaily's sea spectrum, JONSWAP spectrum, PM spectrum, WEN spectrum, etc. [32, 33]. The last three wave spectra are adapted to generate sea surface.

JONSWAP spectrum describes waves that continue to develop in limited wind field:

$$S_{jon}(\omega) = \frac{\alpha g^2}{\omega^5}\exp\left[-\frac{5}{4}\left(\frac{\omega_j}{\omega}\right)^4\right]\gamma^r \#, \quad r = \exp\left[-\frac{(\omega-\omega_j)^2}{2\sigma^2\omega_j^2}\right] \tag{2}$$

where γ is the peak elevation factor. In this paper, $\gamma = 7$ is chosen to represent the narrow-banded spectrum. α is the energy scale factor, ω_p is the spectral peak circular frequency, and σ is the peak shape parameters. $\alpha = 0.076(U_{10}^2/Fg)^{0.22}$, $\omega_j = 22(g^2/U_{10}F)^{1/3}$, $\sigma = 0.07\,(\omega \le \omega_j)$, and $0.09\,(\omega > \omega_j)$. Fetch F is the distance from a lee shore, in this paper, $F = 130000$.

PM spectrum describes a fully developed sea wave:

$$S_{pm}(\omega) = \frac{\alpha g^2}{\omega^5}\exp\left(-\beta\left(\frac{\omega_p}{\omega}\right)^4\right)\#. \tag{3}$$

$\omega = 2\pi f$, $\alpha = 8.1\times10^{-3}$, $\beta = 0.74$, $\omega_p = g/U_{19.5}$, U_{10}, $U_{19.5}$ is the wind speed at a place 10 m, 19.5 m from the sea surface. For most of the air currents over the ocean, $U_{19.5} \approx 1.026 \times U_{10}$.

WEN spectrum is the wave spectrum of China offshore. It can describe the different stages of wind wave growth and adapt to different water depths:

$$S(\omega) = \frac{m_0 p}{\omega_w}\exp\left\{-95\left[\ln\frac{p(5.813-5.137\eta)}{(6.77-1.088p+0.013p^2)(1.307-1.426\eta)}\right]\left(\frac{\omega}{\omega_0}-1\right)^{12/5}\right\} \quad 0 \le \omega \le 1.15\omega_w$$
$$S(\omega) = \frac{m_0}{\omega_w}\frac{(6.77-1.088p+0.013p^2)(1.307-1.426\eta)}{5.813-5.137\eta}\left(\frac{1.15\omega_w}{\omega}\right)^m \quad \omega \ge 1.15\omega_w \#, \tag{4}$$

where ω_0 is spectrum peak frequency, m_0 is zeroth moment, p is peakedness, and η is depth parameter. $\omega_w = 5.72/T_{1/3}$, $m_0 = 1/16H_{1/3}^2$, $p = 95.3H_{1/3}^{1.35}/T_{1/3}^{2.7}$, $\eta = 0.625H_{1/3}/d$ $(0 < \eta < 0.5)$, and $m = 2(2-\eta)$. $H_{1/3}$ and $T_{1/3}$ represent the effective wave height and effective period, respectively.

In order to study the influence of different spectra on the occurrence probability of freak waves, this paper uses the SWOP (stereo wave observation project) directional spectrum uniformly:

$$G(\omega,\theta) = \frac{1}{\pi}\left\{1+\left[0.5+0.82\exp\left(-\frac{(w/w_0)^4}{2}\right)\right]\cos 2\theta + 0.32\exp\left(-\frac{(w/w_0)^4}{2}\right)\right\}\#, \tag{5}$$

where $w_0 = 0.855 \times g/U_{10}$.

When $U_{10} = 7$ m/s, the sea surface is beginning to froth, while more than 30% of the sea surface area is covered with droplet and foam as $U_{10} = 25$ m/s. In this paper, freak waves are generated under the condition of $U_{10} = 13.8$ m/s to reduce the influence of foam on EM scattering calculation.

According to (1), we can generate a huge wave height at a specific location by focusing the energy. Specific ranges of ω and θ are chosen to focus their full energy on raising the wave height. We generate freak waves according to Figure 1 and Figure 2. This paper selects some high-energy areas to focus energy according to the distribution of energy (Figure 2). In order to optimize the calculation, we need to choose an appropriate range, which will be discussed in Section 2.2. Before simulation, we need to test the model. In this paper, the sea surface is simulated, and the correctness of the model is verified by spectral estimation. We use the background waves to estimate the spectrum. Test the model by comparing the fit of the simulated spectrum to the target spectrum. The following is the result of the spectrum estimation:

Figure 3 shows that the fitting effect is very good. We simulate freak waves based on the reliable sea surface model. Numerous studies have shown that the freak wave occurrence may be related to wave energy focusing. For some reasons, the wave energy focuses on a certain location, resulting in giant waves. In this paper, we adjust the energy

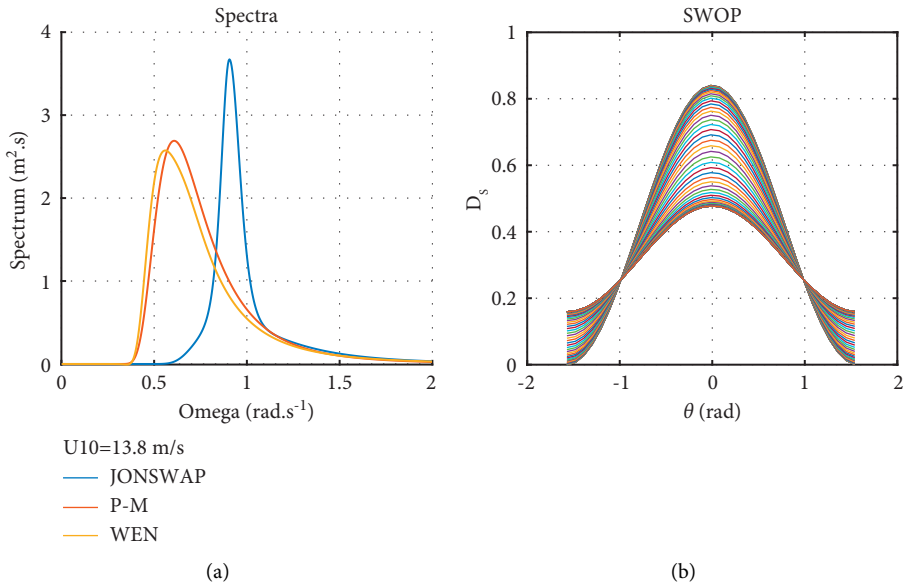

Figure 1: Three kinds of wave spectra and SWOP directional spectrum. (a) JONSWAP spectrum, PM spectrum, WEN spectrum. (b) SWOP directional spectrum.

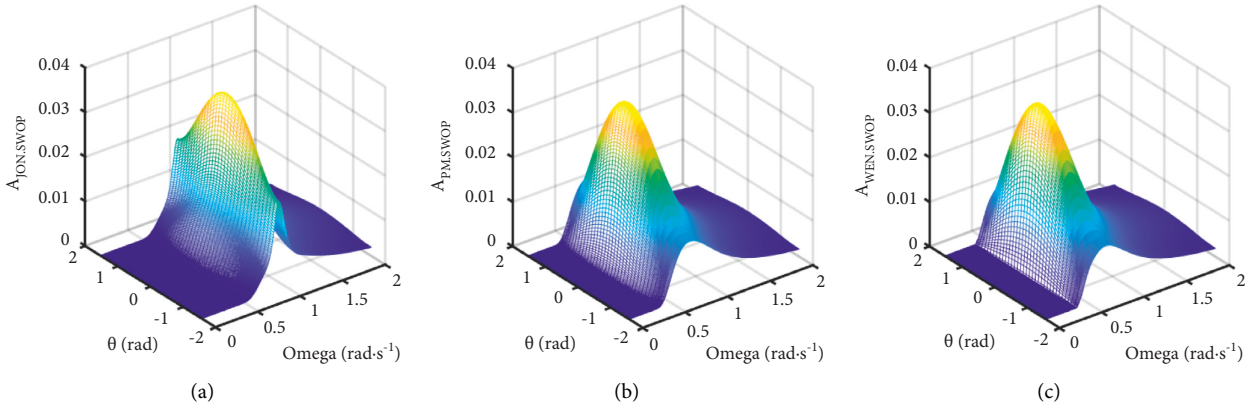

Figure 2: The amplitude of the wavelet. Use the same SWOP spectrum. (a) JONSWAP spectrum. (b) PM spectrum. (c) WEN spectrum.

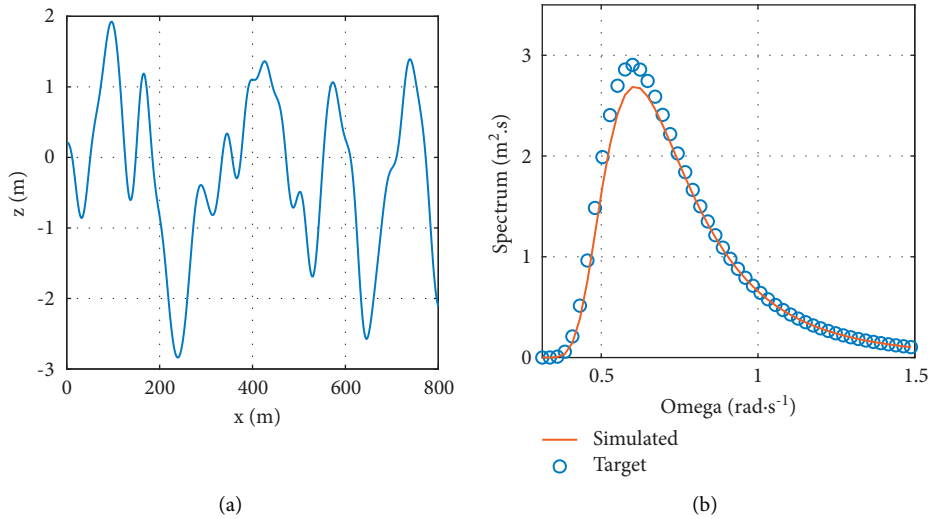

Figure 3: We choose the background wave of the spatial sequence for spectral estimation. (a) A wave waveform selected from the background wave. (b) Spectrum estimation, solid line represents ideal spectrum (target spectrum), circle represents simulation data.

of a part of the wavelets to generate the freak waves at a fixed time and location. It is difficult to judge freak waves and extreme waves by their shapes. Through the above definitions $D_1 \sim D_4$ to determine whether the simulated wave is a freak wave.

We conducted 1000 simulations with different types of sea surface and randomly selected a set of data (Table 1). It can be seen from Figure 4 that the freak wave and the extreme wave are similar in shape. The definitions of freak waves are important. The wave height of the freak wave is not a decisive factor; its value can range from $7 \sim 15$ m, ($U_{10} = 13.8$ m/s). The relationship between adjacent waves is the key to find freak waves. While extremum waves often appear in groups for a long time, the freak wave often appear suddenly alone. The occurrence probability of freak waves is much lower than extreme waves. We strictly follow the definitions when we model freak waves.

2.2. Numerical Simulation of Freak Wave. In this paper, the sea surface of 800×800 m is selected to simulate freak waves. Reduce the amount of calculation and improve the speed of the model while maintaining the wave spectrum structure. With a controlled focusing in both time and space, we decided to use the wave focusing approach, one of the fastest and powerful methods to simulate ideal freak waves. The angular frequency $\omega[0.3, 1.3]$ is divided into 50 parts $[1, 50]$, and the direction angle $\theta[-\pi/2, \pi/2]$ is divided into 35 parts $[1, 35]$. To generate freak waves, we choose the range of wavelets used to focus the energy. Different wave spectra and different wind speeds affect the selection range of wavelets, and a reasonable range directly affects the occurrence of freak waves. The results are as follows.

Freak waves are often accompanied by strong winds. We do not know whether the formation of freak waves is caused by the wind, and how the wind affects the generation of freak waves. Wind speed affects three sea wave spectra, and we study the occurrence probability of freak waves under different winds. Select medium to high wind speed $\{13.8, 17.1, 20.7\}$. Use SWOP direction function. $\theta[10, 18]$ used to focus energy. We have designed some sets of angular frequencies; the frequencies ω in the set are used to focus energy. The selection of elements in the set is the key to fast simulate the freak waves.

The complete freak wave process is an important topic. The duration of the freak wave is very short. We simulated the whole process based on the observed freak wave data. According to the data, we simulated the occurrence process of freak waves for 15s. The disadvantage is that the sea surface does not change with time, which is not a continuous process, for example, Figure 5. The independent time-invariant sea surface at different times helps us to ideally observe each stage of the freak wave, which is also helpful for the subsequent EM scattering calculation. We discuss the range of $\omega[1, 50]$. The results are as follows.

It can be seen from Table 2 that JONSWAP spectrum is more suitable for simulation of freak waves and can adapt to various wind speeds compared with other sea spectra. The

Table 1: Three different types of sea surface. Record the definition of freak wave $D_1 \sim D_4$. Judging freak waves by parameters.

Type	Sea wave	Extreme wave	Freak wave
D_1	1.58	2.85	2.70
D_2	0.58	0.90	0.75
D_3	1.28	1.75	3.79
D_4	2.12	1.03	2.75
	×	×	√

JONSWAP spectrum of $\gamma = 7$ is a typical narrow band spectrum. It is reasonable to use narrow band spectrum for the simulation of freak waves [20]. Observe the shape of the narrow band spectrum; it narrows in both the frequency bandwidth and the directional spreading. The energy is concentrated at the wave crest, and it is easy to focus energy suddenly. Many studies have shown that the occurrence probability of freak waves is closely related to the shape of the wave spectrum [34]. The occurrence probability of freak waves is inhomogeneous in space. Researchers try to link freak wave events to particular meteorological conditions. A high probability freak wave region can be formed under certain synoptic meteorological conditions [20]. Prediction of the freak wave by using wave spectra is a possible and interesting filed [35]. Considering that the wave forecast systems are based on spectral modelling. The formation of narrow band wave spectrum may be a prerequisite for certain meteorological states. The relationship between meteorological states, wave spectrum, and freak waves is the focus of the study.

3. Electromagnetic Scattering Calculation Model of Time-Invariant Freak Wave

The EM scattering characteristic of freak waves is a frontier field. In this paper, we study the EM scattering characteristics of freak waves from time-invariant sea surface and make a preliminary study on this problem under ideal conditions. We discuss this content under ideal conditions.

Radar cross-section (RCS) or normalized radar cross-section (NRCS) represents the scattering ability of the target. It shows the backscattering characteristics of the target and in far field conditions can be expressed as

$$\sigma = \lim_{r \longrightarrow \infty} 4\pi r^2 \frac{\left\langle \left| E_s \right|^2 \right\rangle}{A \left| E_i \right|^2} \#, \tag{6}$$

where r is the distance between scattering body center and electromagnetic wave source. A denotes the illuminated area. E_s and E_i are the incident field and the scattered field, respectively.

For an ideal sea surface with the freak wave, we calculate its specular scattering. KA can be used to simulate EM backscattering from the large-scale sea surface. KA is broadly employed for studying EM scattering from large-scale sea surface due to its advantage of simple and practical KA method; the scattered field at any point within a source-free region bounded by a closed surface can be represented

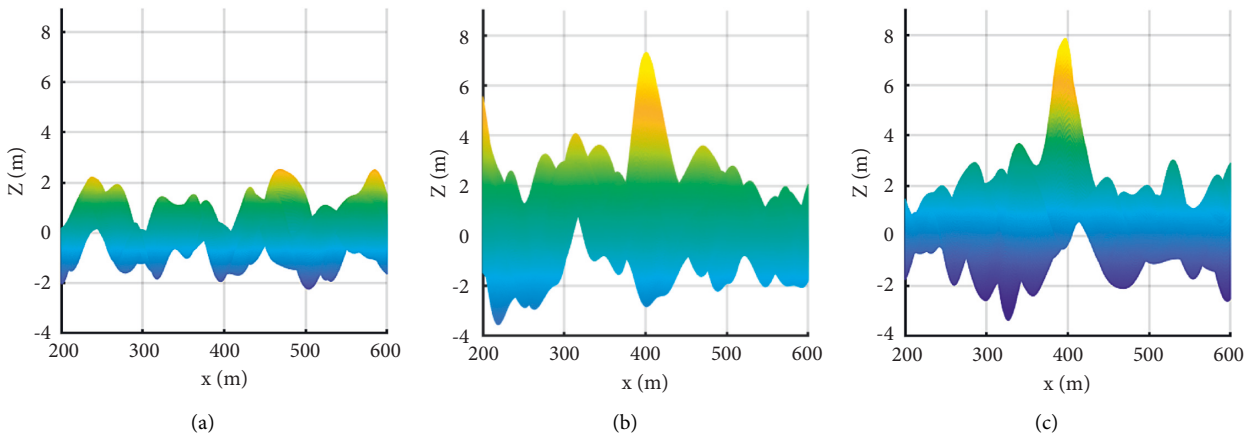

Figure 4: Three different types of sea surface are observed from the sectional shape. (a) Normal seawave. (b) Extreme wave with abnormal wave height. (c) Freak wave.

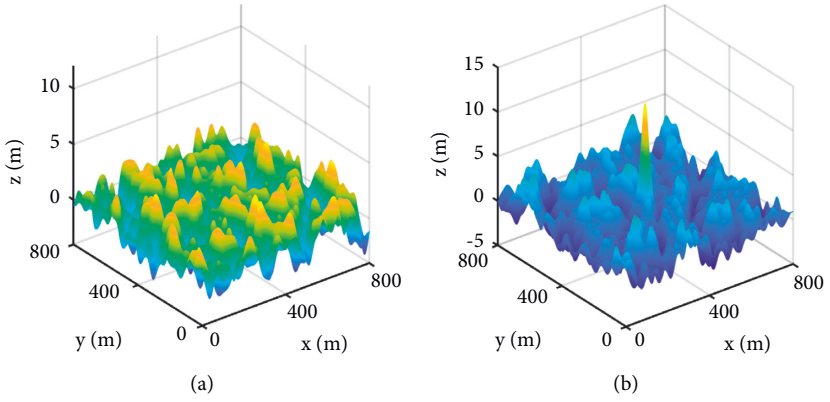

Figure 5: Simulated sea surface 800 × 800. (a) Normal sea surface. (b) Freak wave.

Table 2: The occurrence probability of freak waves under different wind speeds, wave spectra, and wavelet ranges.

Spectral	U_{10}	3–27 (%)	5–29 (%)	7–31 (%)	9–33 (%)	11–35 (%)	13–37 (%)	15–39 (%)	17–41 (%)	19–43 (%)
JONSWAP	13.8	2	18	34	58	70	84	84	86	84
	17.1	16	32	46	64	64	72	68	68	62
	20.7	34	36	48	64	64	64	64	58	40
	13.8	82	90	94	94	88	84	72	48	34
PM	17.1	82	80	64	56	48	24	6	2	1
	20.7	56	48	28	12	4	1	2	1	0
	13.8	88	94	92	90	80	80	62	32	16
WEN	17.1	84	84	60	38	26	10	2	2	1
	20.7	54	38	16	8	1	2	2	1	0

by a tangential field on the surface. The applicable range of KA is

$$\begin{aligned} kl &> 6 \\ R_c &> \lambda \end{aligned} \#, \tag{7}$$

where k is the incidence wave number, l is the correlation length, R_c is the radius of curvature, and λ is the incidence wavelength.

According to the KA, ignoring edge effects such as diffraction, the scattered field is expressed as

$$E_s = \frac{jke^{jkR_0}E_i}{4\pi R_0}\int_{-X}^{X}\int_{-Y}^{Y}\left(a\frac{\partial f(x,y)}{\partial x} + b\frac{\partial f(x,y)}{\partial y} - c\right)e^{j\vec{v}\cdot\vec{r}}\,dx\,dy\#, \tag{8}$$

where $a = (1-R)\sin\theta_i + (1+R)\sin\theta_s\cos\varphi$ and $b = (1+R)\sin\theta_s\sin\varphi$.

$\vec{\mathbf{v}} = k[(\sin\theta_i - \sin\theta_s)\cos\varphi\hat{x} - (\sin\theta_s\sin\varphi)\hat{y} - (\cos\theta_i + \cos\theta_s)\hat{z}]$, θ_i is the incident angle, θ_s is the scattering angle, and φ is the angle between the projection of scattered rays and the $x-axis$.

The reflection coefficient R is the Fresnel reflection coefficient, and, in the case of backscattering, the cross-polarization coefficient is 0. The expression is as follows:

$$\begin{aligned} R^{vv} &= \frac{Y\cos\theta_i - \sqrt{Y\cos\theta_i - \sin^2\theta_i}}{Y\cos\theta_i + \sqrt{Y\cos\theta_i - \sin^2\theta_i}} \\ R^{hh} &= \frac{\cos\theta_i - \sqrt{Y\cos\theta_i - \sin^2\theta_i}}{\cos\theta_i + \sqrt{Y\cos\theta_i - \sin^2\theta_i}} \end{aligned} \#, \tag{9}$$

where Y is the relative permittivity of seawater. $Y = 81.5$ for normal sea water. Substituting (9) into (8), the EM backscattering coefficient is

$$\sigma = \frac{-1}{4XY\cos\theta_i}\left(c + \frac{av_x}{v_z}\right)\int_{-X}^{X}\int_{-Y}^{Y} e^{j(v_x x + v_z f(x,y))}\,dx\,dy\# \tag{10}$$

KA is used to calculate the EM backscattering coefficient from the time-invariant 3D freak waves. C-band SAR is one of the most widely used in ocean observation. This article takes C-band as an example. The freak waves are easier to detect from the background sea surface with HH polarization than with VV polarization. Set simulation parameters: $U_{10} = 13.8$ m/s, 20.7 m/s; the frequency of incident waves is 5.3 GHz; HH polarization; grazing angles θ_g are $40^\circ, 80^\circ$. The results are as follows.

We can ideally observe the various stages of the freak wave, like Figure 6, and calculate each NRCS. Different colors on Figure 7 represent electromagnetic scattering of different intensities. Blue indicates that the backscattered field in this area is relatively weak and is shielded by adjacent waves. Red indicates the backscattered field strength. We compared the NRCS from freak waves under different conditions. Wind speed U_{10} and grazing angle θg have great influence on the numerical simulation. We conducted simulations with different parameters, as follows:

The above figures show the two stages before and after the occurrence of the freak wave. We use different grazing angles to observe. We can see the NRCS difference clearly from Figure 8. T = 2s is the stage when the freak wave is forming. At this stage, the NRCS difference between the freak wave and the background wave is little. It is difficult to capture the freak wave from its initial stage. T = 15s is the stage when the freak wave disappears, and, at this time, there is no obvious difference from the normal sea surface. It is also difficult to capture freak waves from the top view Figure 9. The following is the NRCS under different grazing angles and different wind speeds:

According to the simulation results, we can directly see the EM scattering from the freak waves. There are obvious differences between the Figures 8–11. The EM backscattering (NRCS) from freak waves is significantly different from the background waves (Figure 10). We conducted numerical simulations with different grazing angles and different wind speeds. Observing the change of grazing angle, the NRCS difference between the freak wave and the background wave increases with the increase of the grazing angle. The blue part in the Figure 11 obviously increases, but the shape of the red range indicating the freak wave becomes smaller. With the increase of wind speed, the wave height of the background wave increases, and it becomes difficult to capture the freak wave. The red part under the low grazing angle increased significantly, and the freak wave can be clearly distinguished until the grazing angle is increased. High grazing angles (low incidence angles) make it more possible to detect freak waves.

Freak waves are difficult to capture in practical radar because of its noise characteristics. The real radar image is always very noisy due to the speckle noise. Freak waves are very localized phenomena, of the order of SAR image pixel size. On high resolution radar, the imaging of the freak wave is not obvious, and it is difficult to distinguish from noise. Thus, how this speckle noise (about 10 ~ 20 dB in magnitude) can be distinguished from freak waves is a research topic. We can obtain a value according to the obvious difference between the freak wave and the background wave, like Figures 10 and 11, which is used to distinguish the background wave, noise, and freak wave. According to numerous simulations, we suggest that the NRCS threshold value of the freak wave is 25 ~ 50 dB. Many factors can affect the NRCS threshold value of freak waves, such as significant wave heights in the area, ocean

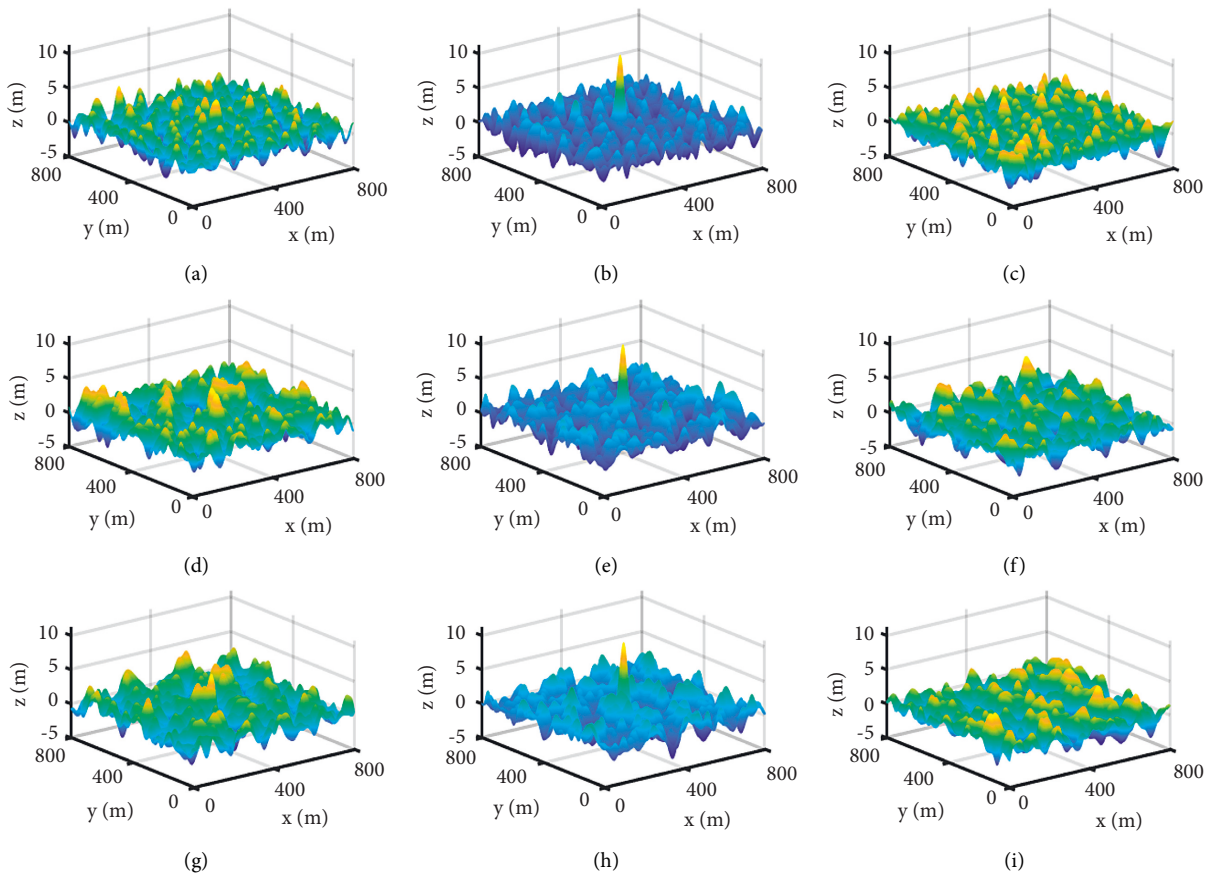

Figure 6: The process of freak waves. Characteristics of each stage. These stages are discontinuous. (a)~(c) Different stages of time-invariant freak waves simulated by JONSWAP spectrum. (d)~(f) Simulated by PM spectrum. (g)~(i) Simulated by WEN spectrum.

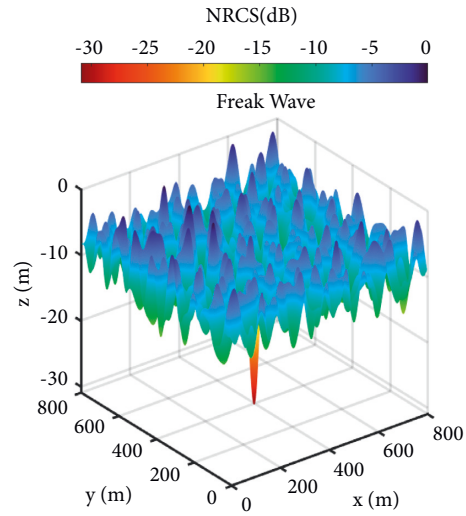

Figure 7: Backscattering (NRCS) from sea surface with the freak wave. U_{10} = 13.8 m/s, $\theta g = 80^{\circ}$.

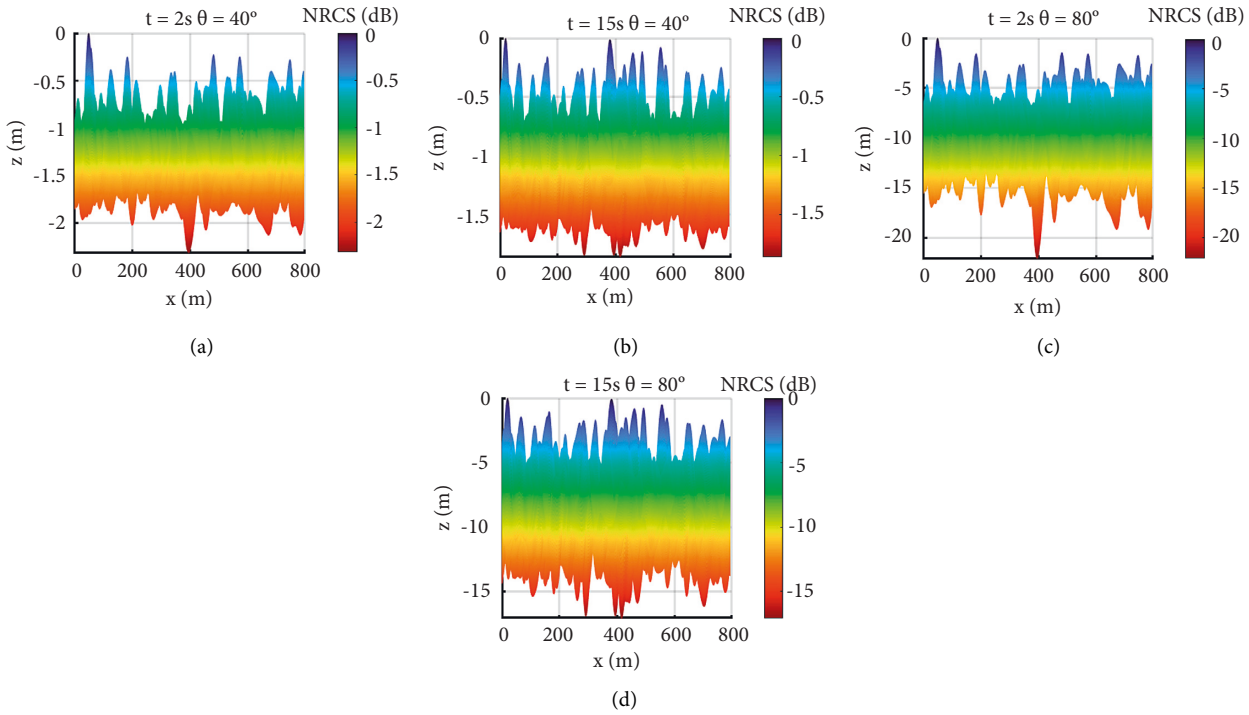

FIGURE 8: X-Z view of NRCS from sea surface with different times and θ. We can clearly see the NRCS difference between the freak wave and the background wave. (a) Preliminary stage of freak wave $\theta = 40^{\circ}$. (b) End stage of freak wave $\theta = 40^{\circ}$. (c) Preliminary stage $\theta = 80^{\circ}$. (d) End stage $\theta = 80^{\circ}$.

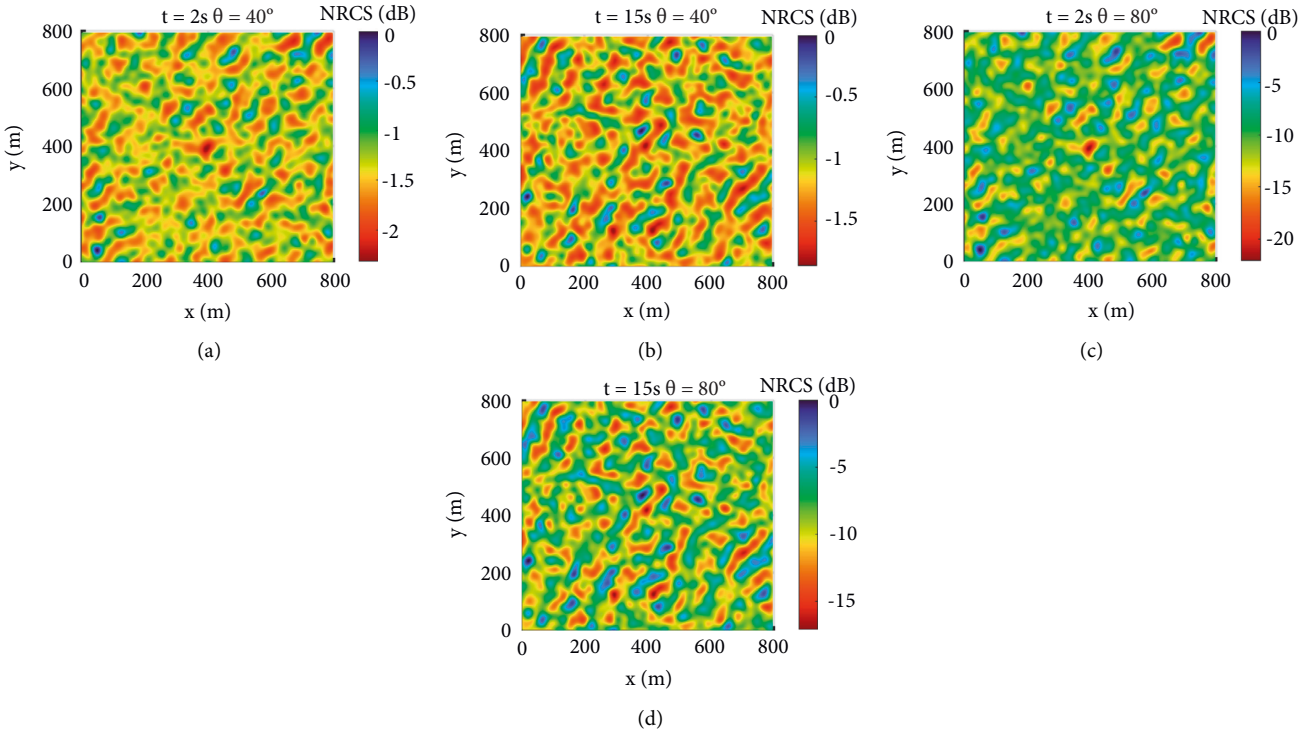

FIGURE 9: X–Y view of NRCS distribution from sea surface with different times and θ. We can see NRCS from the whole sea surface clearly. (a) Preliminary stage of freak wave $\theta = 40^{\circ}$. (b) End stage of freak wave $\theta = 40^{\circ}$. (c) Preliminary stage $\theta = 80^{\circ}$. (d) End stage $\theta = 80^{\circ}$.

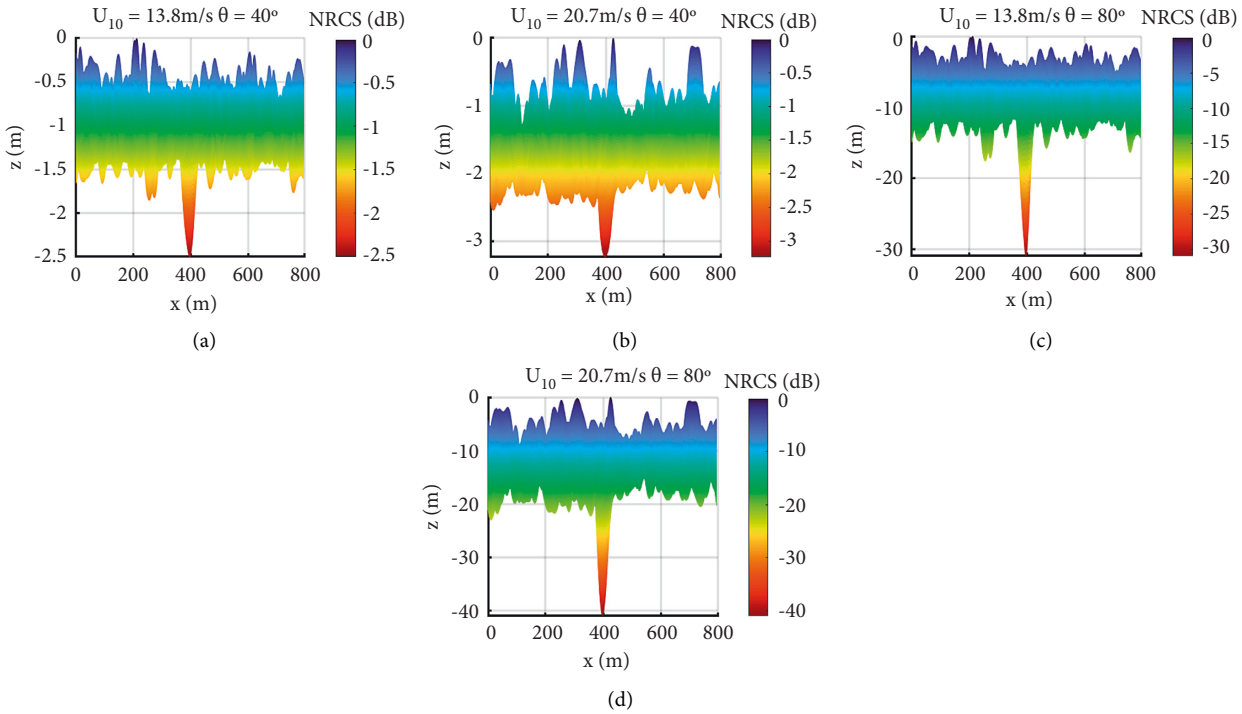

FIGURE 10: X-Z view of NRCS from freak wave sea surface with different U_{10} and θ. (a) U_{10} = 13.8 m/s, $\theta = 40^{\circ}$. (b) U_{10} = 20.7 m/s, $\theta = 40^{\circ}$. (c) U_{10} = 13.8 m/s, $\theta = 80^{\circ}$. (d) U_{10} = 20.7 m/s, $\theta = 80^{\circ}$.

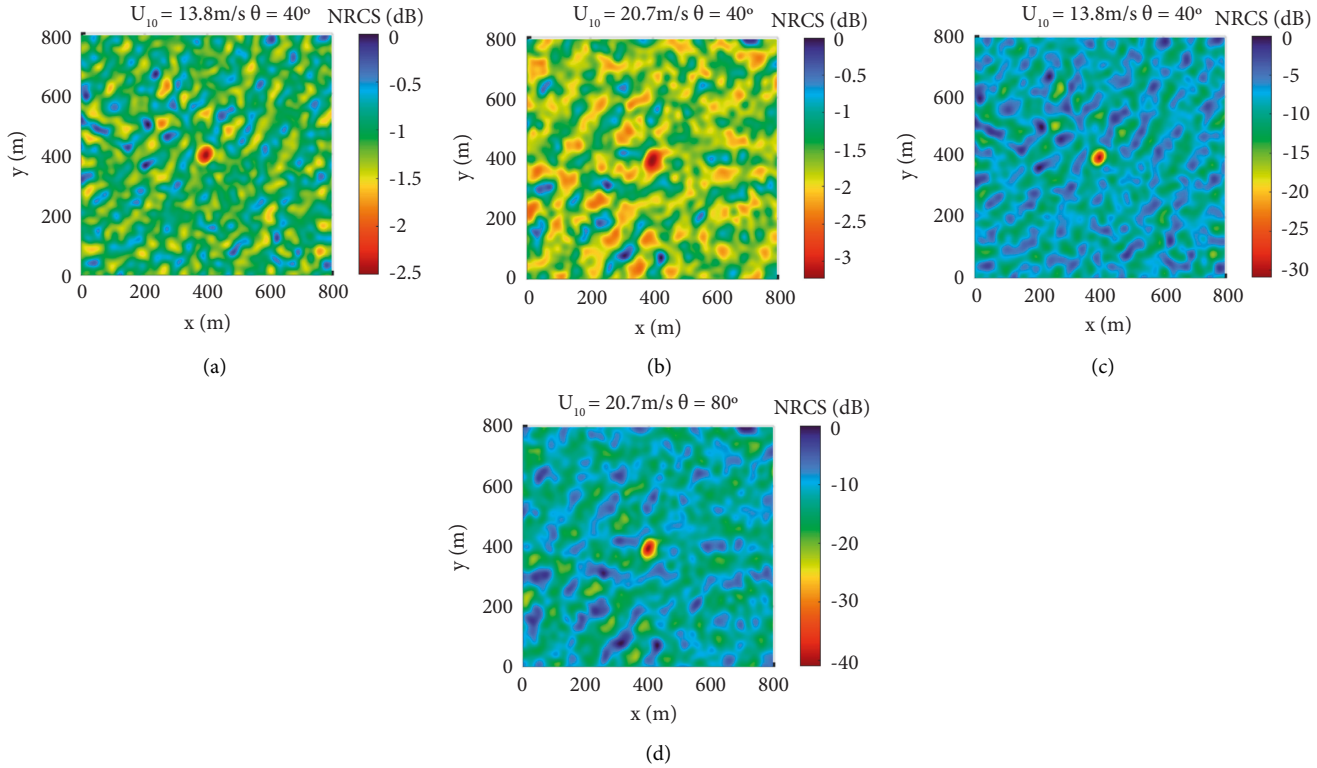

FIGURE 11: X–Y view of NRCS distribution from freak wave sea surface with different U_{10} and θ. (a) U_{10} = 13.8 m/s, $\theta = 40^{\circ}$. (b) U_{10} = 20.7 m/s, $\theta = 40^{\circ}$. (c) U_{10} = 13.8 m/s, $\theta = 80^{\circ}$. (d) U_{10} = 20.7 m/s, $\theta = 80^{\circ}$.

currents, synoptic meteorological, etc. Even the radar itself can affect the threshold value. Dynamically calculating the NRCS threshold value of freak waves is a challenge. The study of EM scattering from sea surface with freak waves is a frontier subject.

4. Conclusions

The 'freak waves' means individual waves with a crest of an extremely high slope compared with background waves. According to the observed freak wave data, we simulated the whole process. This paper discusses the influence of different wave spectra on the simulation of freak waves under different wind speeds. On the validated numerical simulation model of sea surface, the time-invariant 3D freak wave is generated by adjusting the wavelet energy. The numerical simulation shows that the occurrence probability of simulated freak waves is significantly different with different wave spectra under different conditions. The shape of the spectrum affects the occurrence probability of freak waves. The narrow band spectrum is more suitable for the simulation of freak waves. We usually do wave forecast based on spectral modelling, which helps researchers to study the predictability of rogue events by means of probabilistic approaches.

In this paper, we choose JONSWAP spectrum to simulate the freak wave for EM scattering calculation. The EM scattering characteristics of sea surface with freak waves are studied by KA method. The EM backscattering (NRCS) from freak wave and background wave is studied under different grazing angles and different wind speeds. The numerical simulations show that the backscattering coefficients of the freak wave and the background wave are significantly different. The wind speed and the grazing angle have great influence on NRCS. In real observation, it is difficult to find freak waves by defining $D_1 \sim D_4$. Radar echoes can catch them faster and more accurately. We try to use the difference between the NRCS of the background wave and the freak wave as the judgment condition. This theory is feasible under ideal conditions. However, in practical engineering, it is still difficult to distinguish the freak wave from the speckle noise, which makes the identification and capture of the freak wave more difficult. Accurately detecting freak waves on real radar and distinguishing noise is the next topic.

Data Availability

No data were used to support this study.

Conflicts of Interest

The authors declare that they have no conflicts of interest regarding the publication of this paper.

Acknowledgments

This work was supported by the Natural Science Foundation of Shandong Province, China (Grant no. ZR2021MD063).

References

[1] E. Didenkulova, I. Didenkulova, O. Didenkulov, and I. Medvedev, *Analysis of Rogue Wave Events in 2005-2021*, Copernicus Meetings, 2022.

[2] G. K. Wu, C. X. Liu, and Y. Q. Liang, "Computational simulation and modeling of freak waves based on longuet-higgins model and its electromagnetic scattering calculation," *Complexity*, vol. 2020, Article ID 2727681, 14 pages, 2020.

[3] Y. C. Chen and D. J. Doong, "Modeling coastal freak wave occurrence," *Journal of Marine Science and Engineering*, vol. 10, no. 3, p. 323, 2022.

[4] F. L. Huo, H. K. Yang, Z. Yao, K. An, and S. Xu, "Study on slamming pressure characteristics of platform under freak wave," *Journal of Marine Science and Engineering*, vol. 9, no. 11, p. 1266, 2021.

[5] P. N. Sun, M. Luo, D. Le Touzé, and A. M. Zhang, "The suction effect during freak wave slamming on a fixed platform deck: smoothed particle hydrodynamics simulation and experimental study," *Physics of Fluids*, vol. 31, no. 11, Article ID 117108, 2019.

[6] X. Zhao, Z. Ye, Y. Fu, and F. F. Cao, "A CIP-based numerical simulation of freak wave impact on a floating body," *Ocean Engineering*, vol. 87, pp. 50–63, 2014.

[7] Y. F. Deng, J. M. Yang, W. H. Zhao, X. Li, and L. F. Xiao, "Freak wave forces on a vertical cylinder," *Coastal Engineering*, vol. 114, pp. 9–18, 2016.

[8] A. Slunyaev, "Persistence of hydrodynamic envelope solitons: detection and rogue wave occurrence," *Physics of Fluids*, vol. 33, no. 3, Article ID 036606, 2021.

[9] R. L. Fu, Y. X. Ma, G. H. Dong, and M. Perlin, "A wavelet-based wave group detector and predictor of extreme events over unidirectional sloping bathymetry," *Ocean Engineering*, vol. 229, Article ID 108936, 2021.

[10] K. Dysthe, H. E. Krogstad, and P. Müller, "Oceanic rogue waves," *Annual Review of Fluid Mechanics*, vol. 40, no. 1, pp. 287–310, 2008.

[11] Z. Lyu, N. Mori, and H. Kashima, "Freak wave in high-order weakly nonlinear wave evolution with bottom topography change," *Coastal Engineering*, vol. 167, Article ID 103918, 2021.

[12] D. Andrade, R. Stuhlmeier, and M. Stiassnie, "Freak waves caused by reflection," *Coastal Engineering*, vol. 170, Article ID 104004, 2021.

[13] C. Kharif, J. P. Giovanangeli, J. Touboul, L. Grare, and E. Pelinovsky, "Influence of wind on extreme wave events: experimental and numerical approaches," *Journal of Fluid Mechanics*, vol. 594, pp. 209–247, 2008.

[14] T. B. Benjamin and J. E. Feir, "The disintegration of wave trains on deep water. Part 1. Theory," *Journal of Fluid Mechanics*, vol. 27, no. 3, pp. 417–430, 1967.

[15] X. B. Wang and B. Han, "Characteristics of rogue waves on a soliton background in the general three-component nonlinear Schrödinger equation," *Applied Mathematical Modelling*, vol. 88, pp. 688–700, 2020.

[16] Y. Q. Zhang and J. P. Hu, "Effects of high-order nonlinearities on freak wave generation in random sea states," *Journal of Applied Fluid Mechanics*, vol. 15, no. 4, pp. 1221–1229, 2022.

[17] F. Fedele, J. Brennan, S. Ponce de León, J. Dudley, and F. Dias, "Real world ocean rogue waves explained without the modulational instability," *Scientific Reports*, vol. 6, no. 1, pp. 27715–27811, 2016.

[18] I. V. Lavrenov and A. V. Porubov, "Three reasons for freak wave generation in the non-uniform current," *European*

Journal of Mechanics - B: Fluids, vol. 25, no. 5, pp. 574–585, 2006.

[19] L. Zou, A. M. Wang, Z. Wang, Y. G. Pei, and X. L. Liu, "Experimental study of freak waves due to three-dimensional island terrain in random wave," *Acta Oceanologica Sinica*, vol. 38, no. 6, pp. 92–99, 2019.

[20] T. Waseda, M. Hallerstig, K. Ozaki, and H. Tomita, "Enhanced freak wave occurrence with narrow directional spectrum in the North Sea," *Geophysical Research Letters*, vol. 38, no. 13, 2011.

[21] A. V. Babanin, M. Onorato, and L. Cavaleri, "On natural modulational bandwidth of deep-water surface waves," *Fluid*, vol. 4, no. 2, p. 67, 2019.

[22] A. V. Babanin and W. E. Rogers, "Generation and limiters of rogue waves," *The International Journal of Ocean and Climate Systems*, vol. 5, no. 2, pp. 39–49, 2014.

[23] D. Li, B. H. Zhang, and A. G. Shi, "Overview on the study of freak waves and ships encountering with freak waves," *Ship Electronic Engineering*, vol. 36, no. 8, 21 pages, 2016.

[24] G. K. Wu, J. B. Song, and W. Fan, "Electromagnetic scattering characteristics analysis of freak waves and characteristics identification," *Acta Physica Sinica*, vol. 66, no. 13, pp. 134302–134311, 2017.

[25] T. Liu, L. Zhang, Z. G. Zeng, and S. J. Wei, "Study on the composite electromagnetic scattering from 3D conductor multi-objects above the rough surface," *Radioengineering*, vol. 30, no. 2, pp. 323–334.

[26] C. Bourlier and G. Berginc, "Microwave analytical back-scattering models from randomly rough anisotropic sea surface-comparison with experimental data in C and ku bands," *Progress in Electromagnetics Research*, vol. 37, pp. 31–78, 2002.

[27] F. T. Ulaby, R. K. Moore, and A. K. Fung, "Microwave remote sensing: active and passive," *Volume 3-From theory to applications*, vol. 3, 1986.

[28] A. Voronovich, "Small-slope approximation for electromagnetic wave scattering at a rough interface of two dielectric half-spaces," *Waves in Random Media*, vol. 4, no. 3, pp. 337–367, 1994.

[29] H. L. Zheng, J. Zhang, Y. Zhang, A. Khenchaf, and Y. Wang, "A modified TSM for better prediction of hh polarized microwave backscattering coefficient from sea surface," *Remote Sensing Letters*, vol. 11, no. 12, pp. 1137–1146, 2020.

[30] L. Draper, "Freak wave," *Marine Observer*, vol. 35, pp. 193–195, 1965.

[31] P. Klinting and S. E. Sand, *Analysis of Prototype Freak Waves*, pp. 618–632, Costal Hydrody-namics, ASCE, 1987.

[32] T. Elfouhaily, B. Chapron, K. Katsaros, and D. Vandemark, "A unified directional spectrum for long and short wind-driven waves," *Journal of Geophysical Research: Oceans*, vol. 102, no. C7, pp. 15781–15796, 1997.

[33] X. L. Mi, X. B. Wang, X. Y. He, and F. Dai, "sea surface electromagnetic scattering characteristics of JONSWAP spectrum influenced by its parameters CS & IT conference proceedings," *CS & IT Conference Proceedings*, vol. 9, no. 9, 2019.

[34] C. Kirezci, A. V. Babanin, and D. Chalikov, "Probabilistic assessment of rogue wave occurrence in directional wave fields," *Ocean Dynamics*, vol. 71, no. 11-12, pp. 1141–1166, 2021.

[35] O. Gramstad and E. Bitner-Gregersen, "Predicting extreme waves from wave spectral properties using machine learning," *International Conference on Offshore Mechanics and Arctic Engineering*, vol. 58783, 2019.